Lanthanide β-Diketonate Glyme Complexes exhibiting Unusual Co-ordination Modes†

Simon R. Drake,[*,a] **Abigail Lyons,**[b] **David J. Otway,**[a] **Alexandra M. Z. Slawin**[a] **and David J. Williams**[*,a]

[a] *Department of Chemistry, Imperial College of Science, Technology and Medicine, South Kensington, London SW7 2AY, UK*

[b] *Inorgtech, 25 James Carter Road, Mildenhall, Suffolk IP28 7DE, UK*

The reaction of the hydrated β-diketonate complexes [Ln(tmhd)$_3$(H$_2$O)] with triglyme (2,5,8,11-tetraoxadodecane, L^1) in hexane yielded the eight-coordinate triglyme-bridged dimeric complexes, [{Ln(tmhd)$_3$}$_2$L^1] (Ln = Eu **1** or Tb **2**; tmhd = Bu^{t}COCHCOBu^t). In contrast, the reaction of [La(tmhd)$_3$(H$_2$O)] with tetraglyme (2,5,8,11,14-pentaoxapentadecane, L^2) in hexane yielded the nine-co-ordinate monomeric compound [La(tmhd)$_3$L^2] **3**, though with only three of the five possible oxygen atoms of the glyme utilized in bonding to the lanthanum. All of these complexes are air- and moisture-stable and most importantly have good volatility and thermal stability, as demonstrated by sublimation, differential scanning calorimetry and thermal gravimetic analysis. The structures of all three complexes have been determined by single-crystal X-ray diffraction.

The chemistry of lanthanide alkoxides and β-diketonates is in the process of rapid development with many novel molecular compounds reported in the last five years.[1] These materials are of importance as molecular precursors of mixed-metal oxides. The major foreseeable application of such precursors is in the synthesis of electroceramics, *e.g.* superconductors such as $YBa_2Cu_3O_{7-x}$,[2] $Pb_2Sr_2LnCu_3O_{8-x}$[3] and $La_{2-x}Sr_xCuO_4$,[4] piezoelectrics such as $LaCuO_2$,[5] as phosphors[6] and NMR shift reagents, *e.g.* [{Eu(tmhd)$_3$}$_2$] and [{Pr(tmhd)$_3$}$_2$],[7] (Htmhd = 2,2,6,6-tetramethylheptane-3,5-dione).

Multimetallic oxide ceramics are conventionally made by classical 'heat and bake' technology. This approach relies upon the intimate mixing of metal–oxygen based materials (*e.g.* carbonates or nitrates) *via* the use of techniques such as ball milling or hot isostatic pressing. Although attractive owing to its inherent simplicity and low cost, this method has several disadvantages. These are, high-temperature annealing, phase inhomogeneity and the presence of ionic impurities in the product. In contrast, metal alkoxides and β-diketonates have been used because of their advantageous properties.[8] These materials are obtainable as crystalline solids of known stoichiometry, high purity, good solubility in organic solvents, stability in an inert atmosphere, and are sufficiently reactive that most reactions occur at or slightly above room temperature. Most importantly by using such materials fine control of molecular stoichiometry is possible and access to metastable phases may be achieved.

Metal alkoxides and β-diketonates find extensive use in either sol-gel or chemical vapour deposition (CVD) processes, which involve the formation of either thick films (sol-gel spin coatings) or ultrathin films (20 Å or less) for optical or microelectronic applications by CVD. To date conventional lanthanide precursors for such films have several drawbacks, most notably in the high residue left in commercial evaporators/bubblers (for CVD) and poor stability to the atmosphere.

Lanthanide alkoxides and β-diketonates have been well established in the literature for many years,[9,10] and a considerable diversity of β-diketones and Lewis bases has been used to prepare such compounds.[11] These synthetic strategies have all generally used water-soluble salts (*e.g.* chlorides or nitrates) and the most common route utilizes metathesis. A subsequent modification of this, especially where the pK_a of the β-diketonate is not low, is to use a water–ammonia mixture to drive the reaction to completion. Given the inherent simplicity and cheapness of these processes we have sought to capitalize on these routes as a low-cost entry into anhydrous lanthanide β-diketones. Our main criteria are as follows: (*a*) the starting material should preferably be synthesised in aqueous or aqueous–alcohol media; (*b*) the laboratory equipment should be such that if successful industrial scale-up is desired it is easily achievable at low cost; (*c*) most importantly, could materials such as [M(acac)$_3$(H$_2$O)$_n$] (acac = acetylacetonate) prepared *via* the above route be easily converted into water-free products with the desired air/moisture stability and have good volatility/mass transport properties for CVD?

Herein, we report the extension of our tailored molecular-precursor technique, developed for the alkaline-earth-metal β-diketonates,[12] to the related area of the rare-earth-metal β-diketonates, and discuss their thermal stability and possible suitability as CVD precursors.

Experimental

General Procedures.—All manipulations were carried out under an atmosphere of dry (molecular sieves) nitrogen using standard glove-box (Miller-Howe FF 160 with double recirculator system) and Schlenk techniques (using 'greaseless' J. Young's joints/valves). All hydrocarbon solvents were rigorously predried and then distilled first over calcium oxide and then over calcium metal by standard techniques. Elemental analyses were performed by the microanalytical department of Imperial College. The melting points were measured under argon in sealed capillaries and are uncorrected.

Instrumentation.—Infrared spectra were recorded on a Perkin Elmer FTIR 1720 spectrometer as either Nujol or hexachlorobutadiene mulls between 25 × 4 mm CsI plates. The Nujol and hexachlorobutadiene were both predried with 4 Å molecular sieves prior to use (and stored in a glove-box); the samples were

---

† *Supplementary data available:* see Instructions for Authors, *J. Chem. Soc., Dalton Trans.*, 1993, Issue 1, pp. xxiii–xxviii.

Non-SI units employed: Torr ≈ 133 Pa, cal = 4.184 J.

protected from the atmosphere by an O-ring sealed Presslok holder (Aldrich Chemicals). The NMR spectra were recorded on a JEOL GS 270 MHz spectrometer, using the protio impurities of the deuteriated solvent as reference for ^1H spectra and the ^{13}C resonance of the solvent as a reference for ^{13}C spectra. Chemical shifts were also independently referenced to tetramethylsilane (*ca.* 1%) added by volume. All chemical shifts are reported positive to high frequency of the standard. Mass spectra were run on a Kratos MS30 instrument in electron-impact positive-ion mode at the Royal School of Pharmacy Mass Spectrometry Service, University of London.

Cryoscopic measurements were performed in freshly distilled benzene under anaerobic conditions using an electronically controlled thermistor-based apparatus connected to an X–Y chart recorder. All results are an average of at least three measurements. Controlled thermal analysis of the complexes was investigated using a Polymer Laboratories 1500H simultaneous thermal analyser, controlled by a Omni Pro 486DX-33 personal computer connected to a Rioch 1200 laser printer. The mass of the samples investigated was between 9 and 22 mg. The measurements were carried out in alumina crucibles under an atmosphere of flowing (25 cm^3 min^{-1}) nitrogen gas, using heating rates of 5 °C min^{-1}.

Starting Materials.—Nujol and hexachlorobutadiene were obtained from Aldrich Chemicals and dried over 4 Å molecular sieves prior to use. The complexes [Ln(thmd)$_2$(H$_2$O)] (Ln = Eu, La or Tb) were prepared by the literature route.[13] All of the complexes described here are air and moisture stable, but were routinely prepared under nitrogen using thoroughly degassed and dry solvents.

[{(Eu(tmhd)$_3$}$_2$L^1] **1** (L^1 = 2,5,8,11-*tetraoxadodecane, triglyme*). The complex [Eu(tmhd)$_3$(H$_2$O)] (1.40 g, 2 mmol) was dissolved in hexane (10 cm^3) in a Schlenk flask and triglyme (0.36 cm^3, 2 mmol) added; the solution was then allowed to stir for 1 h. The solvent was removed *in vacuo* and the resulting oil kept under vacuum at 65 °C for 1 h. On cooling to room temperature the Schlenk flask was rotated to spread the oil over its surface and then clamped. Crystallization of large clear pale yellow crystals occurred over a period of 3 d, with the Schlenk flask being turned every 24 h to spread the oil and induce further crystallization. Yield: 1.72 g, 97%. *m/z* 693 (20), [Eu(tmhd)$_2$L^1]$^+$; 639 (100), [Eu(tmhd)$_2$(CH$_3$OCH$_2$CH$_2$OCH$_2$CH$_2$OH)]$^+$; 518 (95), [Eu(tmhd)$_2$]$^+$ and [Eu$_2$(tmhd)$_4$]$^{2+}$; and 336 (80%), [Eu(tmhd)]$^+$; *M* 1520 ± 75 (by freezing-point depression in benzene; calc. 1580).

[{Tb(tmhd)$_3$}$_2$L^1] **2**. The complex [Tb(tmhd)$_3$(H$_2$O)] (0.45 g, 0.635 mmol) was dissolved in hexane (10 cm^3) in a Schlenk flask and triglyme (0.115 cm^3, 0.635 mmol) added. The reaction conditions and work-up were as for **1**. Crystallization of large colourless crystals occurs over a period of 24 h. Yield: 0.91 g, 90%. *m/z* 710 (5), [Tb(tmhd)$_3$]$^+$; 703 (3), [Tb(tmhd)$_2$L^1]$^+$; 653 (50), [Tb(tmhd)$_2${Bu^{t}COCHC(H)O}]$^+$; 527 (100), [Tb(tmhd)$_2$]$^+$; 468 (20), [Tb(tmhd){Bu^{t}COCHC(H)O}]$^+$; 426 (8), [Tb(tmhd)(Bu^{t}CO)]$^+$; and 384 (30%), [Tb(tmhd)(MeCHCH$_2$)]$^+$. *M* 1555 ± 84 (by freezing-point depression in benzene, calc. 1594).

[La(tmhd)$_3$L^2] **3** (L^2 = 2,5,8,11,14-*pentaoxapentadecane, tetraglyme*). The complex [La(tmhd)$_3$(H$_2$O)] (0.5 g, 0.74 mmol) was dissolved in hexane (10 cm^3) in a Schlenk flask and tetraglyme (0.15 cm^3, 0.74 mmol) was added. The reaction conditions and work-up were as for **1**. Crystallization of large clear pale yellow crystals of [La(tmhd)$_3$L^2] occurs over a period of 2 d. Yield: 0.61 g, 95%. *m/z* 1148 (4), [La$_2$(tmhd)$_3$(Bu^{t}COCH$_3$)L^2]$^+$; 1030 (4), [La$_2$(tmhd)$_2$L^2{Me(OCH$_2$CH$_2$)$_3$OH}]$^+$; 910 (5), [La(tmhd)$_3$L^2]$^+$; 837 (11), [La(tmhd)$_3$(MeOCH$_2$CH$_2$OCH$_2$CH$_2$OCH$_2$Me)]$^+$; 505 (26), [La(tmhd)$_2$]$^+$; and 323 (16%), [HLa(tmhd)]$^+$. *M* 865 ± 60 (by freezing-point depression in benzene; calc. 911).

Table 1 Crystallographic data for complexes **1** and **3**[a]

	1	**3**
Formula	$C_{74}H_{132}Eu_2O_{16}$	$C_{43}H_{79}LaO_{11}$
M	1580.0	911.0
Colour, habit	Clear blocks	Clear plates
Crystal size/mm	0.30 × 0.40 × 0.53	0.33 × 0.33 × 0.50
Space group	$P2_1/c$	$P2_1/n$
a/Å	20.425(10)	16.010(8)
b/Å	20.280(8)	19.278(8)
c/Å	20.854(10)	17.051(8)
β/°	94.24(4)	106.79(2)
U/Å^3	8614(7)	5038(4)
D_c/g cm^{-3}	1.220	1.201
λ/Å	0.710 73 (Mo-Kα)	1.541 78 (Cu-Kα)
μ/cm^{-1}	14.98 (Mo-Kα)	69.52 (Cu-Kα)
F(000)	3320	1928
Maximum and minimum transmission factors	—	0.4419, 0.1487
No. of unique data	11 930	6795
Observed data	7353 [$F > 4\sigma(F)$]	5112 [$F > 3\sigma(F)$]
2θ range/°	4–46	0–116
Final maximum Δρ/e Å^{-3}	1.69	1.12
Final Δ/σ	1.15	0.060
$R = \Sigma w(F_o - F_c)^2$	0.0673	0.0621
R′	0.0654[a]	0.0582[b]

[a] Details in common: monoclinic; $Z = 4$; scan type $\bar{\omega}$; T 293 K. [b] Weighting function $w^{-1} = \sigma^2(F) + 0.0006F^2$. [c] Weighting function $w^{-1} = \sigma^2(F) + 0.0005F^2$.

Single-crystal X-Ray Analysis.—Single crystals of complexes **1–3** were obtained as outlined above. All of the crystals were subsequently mounted onto glass fibres with epoxy-resin, and were coated with epoxy-resin to reduce any possible crystal decomposition during data collection. The accurate unit-cell parameters for each compound were obtained by means of least-squares analysis of between 18 and 25 centred reflections. Data for compound **1** were collected on a Siemens P4/PC diffractometer using graphite-monochromated Mo-Kα radiation and those for **3** on a Siemens P3/PC diffractometer with graphite-monochromated Cu-Kα radiation. A summary of the crystal data, data collection and refinement parameters is given in Table 1. Two standard reflections were monitored every 50 and showed no significant variation over the data collection. Compound **2** is isostructural with **1** crystallizing in the same crystal system with the same unit cell and space group, *a* = 20.398(8), *b* = 20.240(8), *c* = 20.851(7) Å, β = 94.15(3)°, *U* = 8583(6) Å^3. Structures **1** and **3** were solved by direct methods and refined by full-matrix least squares, using anisotropic thermal parameters for non-hydrogen atoms.[14]

In structure **1** there is disorder in the *tert*-butyl groups attached to C(14) and C(23) associated with the tmhd ligands bound to Eu(1). The carbon atoms of these two groups were refined isotropically with estimated occupancies of 0.4 and 0.6 for the two possible orientations. There is a more complex pattern of disorder in the co-ordination of the tmhd groups to the second europium centre [Eu(2)]. One of these groups is ordered [that associated with O(42) and O(44)], whilst the other two, which co-ordinate to two opposite edges of one of the square faces of the co-ordination polyhedron, are disordered. The disorder is 50:50 between the two pairs of opposite square face edges. As a consequence there is overlap of some partial atom sites but not of others. The atoms with partial occupancies were refined isotropically, those with overlap anisotropically. In both structures the positions of the hydrogen atoms were idealized (C–H 0.96 Å), assigned isotropic thermal parameters [$U_{iso}(H) = 1.2\ U_{eq}(C)$] and allowed to ride on the parent carbon atoms.

The fractional coordinates for complexes **1** and **3** are given in Tables 2 and 4 and selected bond lengths and angles in Tables 3 and 5.

Table 2 Atomic coordinates (× 10^4) for complex **1**

Atom	*x*	*y*	*z*
Eu(1)	2785(1)	−2642(1)	1401(1)
Eu(2)	1984(1)	1177(1)	1291(1)
O(1)	3619(4)	−2007(4)	969(4)
C(1)	4105(5)	−1707(6)	1220(5)
C(2)	4245(8)	−1554(7)	1847(8)
C(3)	3847(6)	−1696(5)	2315(4)
O(3)	3267(5)	−1996(4)	2216(4)
C(4)	4650(4)	−1495(4)	766(4)
C(5)	4434(8)	−1680(9)	75(4)
C(6)	5291(5)	−1848(8)	971(8)
C(7)	4755(8)	−752(5)	813(8)
C(8)	3971(4)	−1527(4)	3050(4)
C(9)	4644(5)	−1207(6)	3172(7)
C(10)	3444(7)	−1051(7)	3246(6)
C(11)	3945(8)	−2158(5)	3444(5)
O(12)	1812(5)	−2524(4)	1879(4)
C(12)	1306(5)	−2897(6)	1959(4)
C(13)	1185(8)	−3494(7)	1678(7)
C(14)	1570(6)	−3753(4)	1225(6)
O(14)	2076(5)	−3524(5)	1049(4)
C(15)	885(4)	−2590(4)	2486(4)
C(16)	649(6)	−1906(4)	2272(6)
C(17)	1304(6)	−2537(8)	3119(4)
C(18)	294(5)	−3030(6)	2576(6)
C(19)	1366(5)	−4439(4)	920(5)
C(20)	1003(11)	−4331(8)	263(7)
C(21)	1978(7)	−4853(7)	844(11)
C(22)	917(10)	−4798(8)	1357(9)
C(20′)	623(5)	−4463(10)	786(16)
C(21′)	1584(16)	−4989(5)	1385(10)
C(22′)	1693(15)	−4529(11)	292(10)
O(23)	3015(5)	−3412(4)	2215(4)
C(23)	3290(6)	−3978(6)	2246(5)
C(24)	3622(7)	−4264(7)	1777(6)
C(25)	3716(5)	−3980(5)	1216(5)
O(25)	3489(4)	−3418(4)	1019(4)
C(26)	3162(5)	−4339(4)	2892(4)
C(27)	3265(11)	−3857(7)	3451(5)
C(28)	2458(6)	−4596(10)	2857(8)
C(29)	3637(9)	−4916(8)	2995(8)
C(27′)	2510(8)	−4108(12)	3124(9)
C(28′)	3714(9)	−4176(12)	3400(6)
C(29′)	3139(15)	−5082(4)	2781(8)
C(30)	4111(4)	−4330(4)	693(4)
C(31)	4588(6)	−3840(6)	427(7)
C(32)	3636(6)	−4579(7)	149(5)
C(33)	4494(7)	−4910(6)	997(6)
C(34)	2552(9)	−2779(8)	−270(7)
O(34)	2327(5)	−2404(5)	250(4)
C(35)	2086(9)	−1782(8)	64(7)
C(36)	1788(9)	−1487(8)	633(8)
O(36)	2292(5)	−1455(4)	1134(4)
C(37)	2164(8)	−1003(6)	1651(7)
C(38)	2607(7)	−442(6)	1656(6)
O(38)	2446(5)	−19(4)	1119(4)
C(39)	2878(8)	−46(4)	639(7)
C(40)	2519(10)	190(9)	38(8)
O(40)	2236(6)	791(5)	158(4)
C(41)	1990(10)	1096(8)	−414(8)
O(42)	2594(4)	2005(4)	793(4)
C(42)	3147(6)	2274(5)	926(6)
C(43)	3597(8)	2089(8)	1405(8)
C(44)	3534(5)	1536(6)	1776(5)
O(44)	3057(4)	1145(4)	1740(5)
C(45)	3239(4)	2878(4)	470(4)
C(46)	3099(8)	2664(8)	−228(4)
C(47)	3942(5)	3132(7)	568(7)
C(48)	2765(7)	3426(5)	624(8)
C(49)	4072(4)	1320(5)	2312(4)
C(50)	4605(6)	1846(7)	2387(8)
C(51)	3759(7)	1234(9)	2948(5)
C(52)	4376(7)	668(6)	2122(8)
O(53)	1822(5)	2032(4)	1953(4)
C(53)	1803(12)	2231(4)	2513(5)
C(53′)	1595(9)	2596(6)	1990(6)
C(54)	1849(14)	1659(5)	2968(9)
C(54′)	1170(14)	2707(11)	1383(9)
C(55)	1771(12)	935(5)	2846(5)
C(55′)	922(11)	2330(9)	797(8)
O(55)	1853(4)	711(4)	2305(4)
C(56)	1808(5)	3000(4)	2616(5)
C(57)	1509(13)	3162(9)	3245(9)
C(58)	2513(7)	3251(12)	2642(14)
C(59)	1408(13)	3330(9)	2060(9)
C(57′)	1644(12)	3726(4)	2504(10)
C(58′)	1440(11)	2742(12)	3174(8)
C(59′)	2455(5)	2923(12)	2774(10)
C(60)	1620(5)	408(5)	3370(4)
C(61)	2142(10)	452(12)	3930(9)
C(62)	948(7)	546(11)	3611(10)
C(63)	1627(12)	−279(5)	3077(9)
C(61′)	1505(13)	−292(7)	3602(9)
C(62′)	2340(6)	590(12)	3510(8)
C(63′)	1192(10)	885(11)	3718(9)
O(64)	1028(4)	540(4)	1173(4)
C(64)	447(4)	659(6)	997(8)
C(64′)	661(5)	348(10)	1582(4)
C(65)	173(8)	1292(6)	723(11)
C(65′)	791(7)	251(11)	2292(5)
C(66)	618(5)	1830(5)	525(8)
C(66′)	1436(6)	449(10)	2624(4)
O(66)	1211(5)	1807(5)	699(5)
C(67)	−27(4)	129(4)	1262(4)
C(68)	−737(3)	338(8)	1104(10)
C(69)	93(9)	−536(5)	952(9)
C(70)	106(10)	72(10)	1989(4)
C(68′)	−474(6)	−66(10)	1784(7)
C(69′)	−335(9)	698(7)	870(9)
C(70′)	63(9)	−459(7)	822(8)
C(71)	393(5)	2519(5)	239(5)
C(72)	−319(7)	2473(9)	−34(12)
C(73)	452(12)	3038(7)	767(9)
C(74)	827(11)	2709(10)	−295(9)
C(72′)	363(14)	3267(5)	172(13)
C(73′)	583(11)	2216(13)	−389(6)
C(74′)	−276(8)	2259(14)	396(13)

Additional material available from the Cambridge Crystallographic Data Centre comprises H-atom coordinates, thermal parameters and remaining bond lengths and angles.

Results and Discussion

Synthesis.—We have found that the reaction of the hydrated β-diketonate complexes [Ln(tmhd)$_3$(H$_2$O)] with 1 equivalent of triglyme (L^1) in hexane at room temperature yields [equation (1)] dimeric complexes containing triglyme, [{Ln(tmhd)$_3$}$_2$L^1] (Ln = Eu **1** or Tb **2**). We have also noted the generality of this reaction with triglyme and a range of [Ln(tmhd)$_3$(H$_2$O)] complexes to yield the same products (Ln = La, Y or Tm).[15]

$$2[\mathrm{La(tmhd)_3(H_2O)}] + 2\mathrm{L}^1 \longrightarrow [\{\mathrm{La(tmhd)_3}\}_2\mathrm{L}^1] + \mathrm{L}^1 + 2\mathrm{H_2O} \quad (1)$$

In contrast to complexes **1** and **2** the reaction of [La(tmhd)$_3$(H$_2$O)] with 1 equivalent of tetraglyme (L^2) yields [equation (2)] the monomeric complex [La(tmhd)$_3$L^2] **3** (see Experimental section). The reaction with tetraglyme and [Ln(tmd)$_3$(H$_2$O)] (Ln = Eu or Tb) complexes also yields

$$[\mathrm{La(tmhd)_3(H_2O)}] + \mathrm{L}^2 \longrightarrow [\mathrm{La(tmhd)_3L^2}] + \mathrm{H_2O} \quad (2)$$

monomeric $[Ln(tmhd)_3L^2]$ compounds.[16] Rather intriguing is the observation that the reaction occurs with the complete elimination of the co-ordinated water molecules. Analysis of the remaining material shows it to be rich in water and excess of tetraglyme. This observation suggests that the glyme ligands are acting as partitioning agents, which is also consistent with the observed reaction stoichiometry. This requires 1 molar equivalent of glyme O-donor ligand, rather than the expected 0.5 equivalent incorporated into the products. The water is removed with only 1 equivalent of glyme in excess. It should be noted however that glymes have previously been used as dehydrating agents for metal chloride hydrates, *e.g.* 2,2-dimethoxypropane reacts with metal hydrates producing acetone and methanol. These by-products are often found complexed to the metal halide;[17] we note that with the longer-chain glymes (*i.e.* tri- or tetra-glyme), no ligand cleavage is observed (from IR, ^1H and ^{13}C NMR spectroscopic data, see Experimental section).

Table 3 Selected bond lengths (Å) and angles (°) for complex **1**

Eu(1)–O(1)	2.367(9)	Eu(1)–O(3)	2.308(8)
Eu(1)–O(12)	2.301(10)	Eu(1)–O(14)	2.383(9)
Eu(1)–O(23)	2.328(8)	Eu(1)–O(25)	2.313(9)
Eu(1)–O(34)	2.557(9)	Eu(1)–O(36)	2.653(9)
Eu(2)–O(38)	2.636(9)	Eu(2)–O(40)	2.577(10)
Eu(2)–O(42)	2.375(9)	Eu(2)–O(44)	2.319(9)
Eu(2)–O(53)	2.256(9)	Eu(2)–O(55)	2.349(8)
Eu(2)–O(64)	2.339(8)	Eu(2)–O(66)	2.317(10)
O(1)–Eu(1)–O(3)	72.1(3)	O(1)–Eu(1)–O(12)	141.0(3)
O(3)–Eu(1)–O(12)	87.5(3)	O(1)–Eu(1)–O(14)	136.8(3)
O(3)–Eu(1)–O(14)	150.4(3)	O(12)–Eu(1)–O(14)	71.7(3)
O(1)–Eu(1)–O(23)	122.1(3)	O(3)–Eu(1)–O(23)	78.0(3)
O(12)–Eu(1)–O(23)	83.5(3)	O(14)–Eu(1)–O(23)	78.8(3)
O(1)–Eu(1)–O(25)	75.9(3)	O(3)–Eu(1)–O(25)	113.5(3)
O(12)–Eu(1)–O(25)	143.0(3)	O(14)–Eu(1)–O(25)	76.3(3)
O(23)–Eu(1)–O(25)	72.5(3)	O(1)–Eu(1)–O(34)	76.3(3)
O(3)–Eu(1)–O(34)	133.7(3)	O(12)–Eu(1)–O(34)	96.8(3)
O(14)–Eu(1)–O(34)	71.3(3)	O(23)–Eu(1)–O(34)	148.3(3)
O(25)–Eu(1)–O(34)	89.9(3)	O(1)–Eu(1)–O(36)	72.5(3)
O(3)–Eu(1)–O(36)	76.9(3)	O(12)–Eu(1)–O(36)	70.7(3)
O(14)–Eu(1)–O(36)	113.8(3)	O(23)–Eu(1)–O(36)	144.5(3)
O(25)–Eu(1)–O(36)	141.4(3)	O(34)–Eu(1)–O(36)	61.6(3)
O(38)–Eu(2)–O(40)	59.9(3)	O(38)–Eu(2)–O(42)	112.7(3)
O(40)–Eu(2)–O(42)	70.5(3)	O(38)–Eu(2)–O(44)	72.0(3)
O(40)–Eu(2)–O(44)	96.6(4)	O(42)–Eu(2)–O(44)	71.7(3)
O(38)–Eu(2)–O(53)	149.3(3)	O(40)–Eu(2)–O(53)	147.5(3)
O(42)–Eu(2)–O(53)	80.2(3)	O(44)–Eu(2)–O(53)	87.3(3)
O(38)–Eu(2)–O(55)	79.5(3)	O(40)–Eu(2)–O(55)	138.3(3)
O(42)–Eu(2)–O(55)	141.0(3)	O(44)–Eu(2)–O(55)	78.0(3)
O(53)–Eu(2)–O(55)	74.1(3)	O(38)–Eu(2)–O(64)	77.5(3)
O(40)–Eu(2)–O(64)	87.6(3)	O(42)–Eu(2)–O(64)	143.6(3)
O(44)–Eu(2)–O(64)	141.6(3)	O(53)–Eu(2)–O(64)	109.2(3)
O(55)–Eu(2)–O(64)	73.9(3)	O(38)–Eu(2)–O(66)	132.2(3)
O(40)–Eu(2)–O(66)	81.5(4)	O(42)–Eu(2)–O(66)	74.7(3)
O(44)–Eu(2)–O(66)	144.8(3)	O(53)–Eu(2)–O(66)	77.1(4)
O(55)–Eu(2)–O(66)	125.7(3)	O(64)–Eu(2)–O(66)	73.5(3)

Table 5 Bond lengths (Å) and angles (°) for complex **3**

La–O(2)	2.706(7)	La–O(5)	2.781(6)
La–O(8)	2.751(7)	La–O(17)	2.495(6)
La–O(19)	2.442(5)	La–O(22)	2.470(7)
La–O(24)	2.481(6)	La–O(27)	2.403(6)
La–O(29)	2.487(6)		
O(2)–La–O(5)	59.5(2)	O(2)–La–O(8)	118.1(2)
O(5)–La–O(8)	58.7(2)	O(2)–La–O(17)	76.4(2)
O(5)–La–O(17)	67.1(2)	O(8)–La–O(17)	78.7(2)
O(2)–La–O(19)	141.2(2)	O(5)–La–O(19)	118.2(2)
O(8)–La–O(19)	71.9(2)	O(17)–La–O(19)	68.9(2)
O(2)–La–O(22)	78.7(2)	O(5)–La–O(22)	128.5(2)
O(8)–La–O(22)	144.5(2)	O(17)–La–O(22)	75.3(2)
O(19)–La–O(22)	76.3(2)	O(2)–La–O(24)	74.7(2)
O(5)–La–O(24)	121.6(2)	O(8)–La–O(24)	144.8(2)
O(17)–La–O(24)	136.0(2)	O(19)–La–O(24)	120.2(2)
O(22)–La–O(24)	67.0(2)	O(2)–La–O(27)	144.6(2)
O(5)–La–O(27)	123.4(2)	O(8)–La–O(27)	76.9(2)
O(17)–La–O(27)	138.9(2)	O(19)–La–O(27)	72.3(2)
O(22)–La–O(27)	108.2(2)	O(24)–La–O(27)	76.4(2)
O(2)–La–O(29)	83.7(2)	O(5)–La–O(29)	67.5(2)
O(8)–La–O(29)	75.4(2)	O(17)–La–O(29)	134.5(2)
O(19)–La–O(29)	133.5(2)	O(22)–La–O(29)	139.9(2)
O(24)–La–O(29)	73.7(2)	O(27)–La–O(29)	68.7(2)

Table 4 Atomic coordinates (× 10^4) for complex **3**

Atom	*x*	*y*	*z*
La	118(1)	2 270(1)	7 968(1)
C(1)	1 624(8)	3 662(7)	7 872(10)
O(2)	1 538(5)	3 103(4)	8 325(5)
C(3)	2 123(9)	3 086(7)	9 099(10)
C(4)	2 236(7)	2 451(9)	9 491(7)
O(5)	1 449(4)	2 099(3)	9 420(4)
C(6)	1 530(9)	1 448(8)	9 774(8)
C(7)	719(8)	1 174(7)	9 800(7)
O(8)	61(4)	1 226(3)	9 052(4)
C(9)	−685(8)	791(5)	8 931(6)
C(10)	−1 257(7)	987(6)	9 454(8)
O(11)	−892(5)	781(4)	10 262(5)
C(12)	−1 417(10)	1 005(9)	10 775(9)
C(13)	−899(10)	1 018(10)	11 601(9)
O(14)	−1 368(8)	1 254(9)	12 111(8)
C(15)	−1 095(12)	1 780(8)	12 536(13)
C(16)	2 294(6)	815(5)	7 343(6)
C(161)	2 703(7)	404(7)	8 109(8)
C(162)	2 799(8)	1 480(6)	7 366(9)
C(163)	2 325(7)	407(6)	6 580(7)
C(17)	1 337(6)	993(4)	7 332(5)
O(17)	1 305(3)	1 491(3)	7 814(4)
C(18)	649(6)	630(4)	6 865(6)
C(19)	−230(5)	754(4)	6 810(5)
O(19)	−481(3)	1 235(3)	7 179(3)
C(20)	−967(6)	287(5)	6 280(6)
C(201)	−650(8)	−334(6)	5 926(8)
C(202)	−1 502(10)	730(7)	5 598(9)
C(203)	−1 490(8)	30(7)	6 821(8)
C(21)	331(7)	2 841(6)	5 269(6)
C(211)	1 249(10)	2 991(14)	5 495(10)
C(212)	159(15)	2 129(7)	5 036(10)
C(213)	−124(11)	3 270(9)	4 541(8)
C(22)	38(6)	2 975(5)	6 032(6)
O(22)	240(4)	2 525(3)	6 585(4)
C(23)	−402(7)	3 600(4)	6 108(7)
C(24)	−583(6)	3 801(5)	6 836(7)
O(24)	−444(4)	3 435(3)	7 462(4)
C(25)	−950(7)	4 533(5)	6 891(8)
C(251)	−1 187(13)	4 929(7)	6 088(11)
C(252)	−1 740(10)	4 488(6)	7 144(12)
C(253)	−303(11)	4 928(7)	7 514(13)
C(26)	−2 918(6)	2 427(5)	7 670(7)
C(261)	−3 028(10)	2 623(11)	6 813(11)
C(262)	−3 523(8)	2 823(12)	7 985(16)
C(263)	−3 140(8)	1 696(7)	7 658(12)
C(27)	−1 947(5)	2 539(4)	8 153(6)
O(27)	−1 405(3)	2 207(3)	7 884(3)
C(28)	−1 709(5)	2 984(4)	8 819(5)
C(29)	−864(6)	3 120(4)	9 288(5)
O(29)	−192(3)	2 873(3)	9 143(3)
C(30)	−674(6)	3 596(5)	10 041(5)
C(301)	−1 331(8)	4 188(6)	9 937(8)
C(302)	−698(9)	3 139(6)	10 770(6)
C(303)	224(8)	3 934(6)	10 219(8)

Table 6 Selected IR data (cm^{-1}) for complexes **1**–**3**

Complex	ν(C–H)[a]	ν(C⩦O)[b]	ν(C⩦C)[b]	δ(C–H)[a]	ν(C–O)[b]	ν(M–O)[b]
1	2962, 2902,	1608	1575	1452, 1421,	1138	406
	2866	1588	1505	1388, 1359		
		1536				
2	2962, 2902,	1609	1574	1452, 1422,	1131	408
	2866	1589	1505	1388, 1359		
		1536				
3	2950, 2924,	1609	1574	1451, 1416,	1136	402
	2900, 2874	1587	1504	1388, 1358		
		1535				

[a] Hexachlorobutadiene mull. [b] Nujol mull.

Table 7 Selected ^{1}H and ^{13}C NMR spectroscopic data for complexes **1** and **3**

Compound	^{1}H[a]	^{13}C[b]
1[c]	−0.55 (s, 54 H)	−5.20 (s, OMe, C^a)
	−0.35 (s, 3 H, H^a)	28.21 (s, Me), 43.46 (s, *C*Me$_3$)
	8.99 (s, 2 H)	75.33 (s, OCH$_2$, C^b)
	10.26 (s, 2 H, H^b)	93.48 (s, CH)
	11.05 (m, 4 H, H^{c,d})	102.26 (s, OCH$_2$, C^{c,d})
		189.48 (s, CO)
3[d]	1.18 (s, 54 H)	28.39 (s, Me), 40.27 (s, *C*Me$_3$)
	3.09 (s, 6 H, H^a)	58.28 (s, OMe, C^a)
	3.26 (m, 4 H, H^b)	70.30 (s, OCH$_2$, C^b)
	3.41 (m, 4 H, H^c)	70.60 (s, OCH$_2$, C^{c,d})
	3.43 (m, 4 H, H^d)	71.81 (s, OCH$_2$, C^e)
	3.46 (s, 4 H, H^e)	89.71 (s, CH),
	5.74 (s, 2 H)	197.61 (s, CO)

[a] All spectra run in C_6D_6 at 270 MHz. [b] All spectra run at 67.94 MHz in C_6D_6. [c] Assignments for triglyme: $(C^aH_3OC^bH_2C^cH_2OC^dH_2)_2$. [d] Assignments for tetraglyme: $(C^aH_3OC^bH_2C^cH_2OC^dH_2C^eH_2)_2O$.

Spectroscopic and Physical Data.—The complexes **1**–**3** were studied as both hexachlorobutadiene and Nujol mulls between CsI windows. Selected IR bands are in Table 6. The bands are tentatively assigned on the basis of the data for the previously characterized hydrated and anhydrous β-diketonates.[16] In the region 1500–1600 cm^{-1}, bands at 1609, 1586 and 1540 cm^{-1} are assigned to the ν(C⩦O) stretching modes and the bands at 1575 and 1500 cm^{-1} to the ν(C⩦C) stretching modes. The metal–oxygen (tmhd) stretching frequencies are assigned at 405 cm^{-1} and our data are in good accord with previous results.[18]

The ^{1}H and ^{13}C NMR spectra of complexes **1** and **3** were run in C_6D_6. For **1** a considerable degree of peak shifting and line broadening was apparent and this is undoubtedly due to the paramagnetic Eu^{3+}, but tentative peak assignments were still possible (see Table 7). Compounds of the type [{Ln(tmhd)$_3$}$_2$] have been used as shift reagents to help simplify complex NMR spectra and as such the shifts above are well precedented.[19] In contrast for **3** a well resolved ^{1}H NMR spectrum was observed (see Table 7), with the expected integration for the different CH$_3$, CH$_2$ and CH environments being observed. From these data it would appear that the tetraglyme is sited in a symmetrical position around the metal nucleus in solution or alternatively that we are observing a time-averaged environment at room temperature. The latter explanation seems most likely given the known weak M–O bonds of O-glyme donors to hard metal centres, such as lanthanides or alkaline-earth metals.

The positive-ion mass spectra of complexes **1**–**3** show some interesting features. The major peak for **1** corresponds to the ion [Eu(tmhd)$_2$(CH$_3$OCH$_2$CH$_2$OCH$_2$CH$_2$OH)]$^+$ at *m*/*z* 639 with some decomposition of the glyme ligand having occurred; above this mass is observed a weaker ion at *m*/*z* 693 corresponding to [Eu(tmhd)$_2$L^1]$^+$. At lower mass a peak for [Eu(tmhd)$_2$]$^+$ at *m*/*z* 518 is noted and [Eu(tmhd)]$^+$ is observed at *m*/*z* 336. Similar behaviour is observed for complex **2**. It is noticeable in the mass spectra of both complexes that the dimeric parent complexes do not remain intact, instead mononuclear fragments containing both tmhd and glyme ligands are observed.

The lanthanum complex [La(tmhd)$_3$L^2] **3** shows several distinct features in its mass spectrum. The monomeric species is observed as a weak molecular ion at *m*/*z* 910; rather surprising is the observation of higher-molecular-weight ions, indicating that this species aggregates in the gas phase to yield dimeric species, *e.g.* [La$_2$(tmhd)$_3$(Bu^{t}COCH$_3$)L^2]$^+$ at *m*/*z* 1148 and [La$_2$(tmhd)$_2$L^2{Me(OCH$_2$CH$_2$)$_3$OH}]$^+$ at *m*/*z* 1030. This observation is noticeably different to that for [{La(tmhd)$_3$}$_2$] where the highest-molecular-mass species was found to be [La(tmhd)$_2$]$^+$.[20]

The determination of the freezing-point depression in benzene gives a molecular weight of 1520 for the europium dimer **1**, very close to the calculated mass of 1580. A similar result was found for the related terbium compound **2**. In contrast the complex [La(tmhd)$_3$L^2] **3** gives a mass of 865 in good agreement with its formulation as a monomeric species (911 expected).

These compounds all have excellent solubility in an extensive range of organic solvents (see Table 8), most likely due to the coordinative saturation of the metal centres. A further important observation (especially if these materials are to have industrial applications) is their excellent stability to both air and moisture (over 3–6 months).

Both compounds **1** and **2** show a significant drop in their melting points of approximately 60 °C on complexation of the glyme ligand (compare parent hydrates, Table 8). Complex **1** has a m.p. of 111–114 °C, and may be contrasted with the hydrated starting compound which melts over the range 174–179 °C. Complex **2** melts at 86–89 °C, and the corresponding hydrate at 147–150 °C; **3** melts at 180 °C below the hydrate (41–44 *cf.* 222–224 °C). These data may be compared with those for the monopyridine adducts [Ln(tmhd)$_3$(py)] (for Eu, 135–138; for Tb, 135–137 °C) which also reveal a reduction in their melting point when compared to the hydrated parent complexes [Ln(tmhd)$_3$(H$_2$O)].[21] With the more bulky nitrogen Lewis base pyrazine, monoadducts are also formed, *e.g.* [Ln(tmhd)$_3$(C$_4$H$_4$N$_2$)] which have a thermal stability akin to those of the hydrated β-ketonate compounds.[22]

Complex **1** sublimes (intact) slowly at 115–130 °C (< 10^{-3} Torr) forming colourless crystals on the cold-finger; at higher temperatures (130–140 °C) it sublimes rapidly yielding a microcrystalline solid. The terbium compound **2** also sublimes intact, over the range 110–130 °C (< 10^{-3} Torr). The lanthanum complex **3** decomposes at 175–195 °C at 10^{-3} Torr to yield the glyme-free homoleptic complex [{La(tmhd)$_3$}$_2$].

DSC/TGA.—Thermal gravimetric analysis (TGA) measurements have found extensive application where a study of weight loss *versus* temerature can give important insight into the breakdown and thermal behaviour of materials at elevated temperature. Differential scanning calorimetry (DSC) allows the study of the enthalpy change occurring during the

Table 8 Selected microanalytical, solubility and melting point data for complexes **1**–**3**

	Microanalysis (%)[a]		Solubility[b]						
Compound	C	H	Ethers	Aromatics	Alkanes	Others	M.p. (°C)[c]	Stability[d]	Volatility[e]
1 [{Eu(tmhd)$_3$}$_2$L^1]	55.8 (56.2)	8.2 (8.4)	V. soluble	V. soluble	V. soluble	V. soluble in Me$_2$SO	111–114	V. stable	115–140
2 [{Tb(tmhd)$_3$}$_2$L^1]	55.3 (55.7)	8.2 (8.3)	V. soluble	V. soluble	V. soluble	V. soluble in Me$_2$SO	86–89	V. stable	110–130
3 [La(tmhd)$_3$L^2]	57.0 (56.7)	8.5 (8.7)	V. soluble	V. soluble	V. soluble	V. soluble in Me$_2$SO	41–44	V. stable	Decomp. to [{La(tmhd)$_3$}$_2$] at 175–195

[a] The calculated values are in parentheses. [b] Typical solvents are diethyl ether, tetrahydrofuran, benzene, toluene, hexane or heptane. [c] Uncorrected values, and tubes sealed under argon. [d] Stability to air/moisture. [e] All sublimations (*T*/°C) at 10^{-3} Torr.

thermolysis and also whether a reaction is occurring (*i.e.* phase change or melting point) or chemical change (irreversible decomposition).[23]

The DSC curve for complex **1** (Fig. 1) shows a sharp reversible melting point of 128.17 °C (−7.14 mcal mg^{-1}) whereas that for the hydrated starting material shows a melting point 65 °C higher at 192.78 °C (−23 mcal mg^{-1}). Both compounds undergo sublimation above 250 °C. The TGA curve shapes for **1** (Fig. 2) and its related hydrate are very similar, with **1** showing the lower onset temperature at 165 °C with completion by 287 °C. In contrast the hydrate has an onset of 180 °C with completion at 295 °C. Over this temperature range, 97 ± 2% of both materials vaporizes into the nitrogen stream leaving a very small (*ca.* 1%) residue.

The DSC curve of compound **2** shows a sharp, reversible melting point centred at 115 °C (−5.10 mcal mg^{-1}), whereas that for the hydrated starting material shows a melting point 50 °C higher at 165 °C (−18.13 mcal mg^{-1}). The TGA curves of compound **2** and of the hydrated complex are very similar to that of complex **1**.

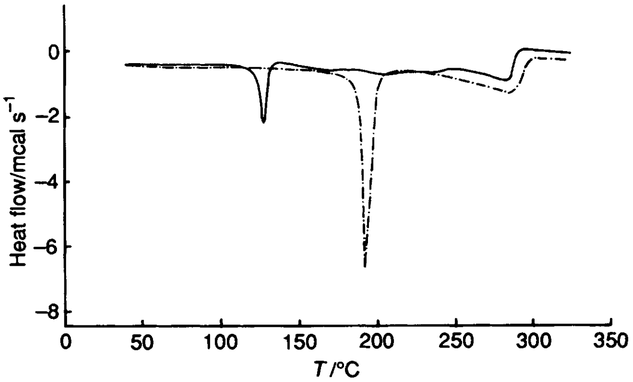

Fig. 1 Differential scanning calorimetry curves for compound **1** (——) and its related hydrate (· — ·)

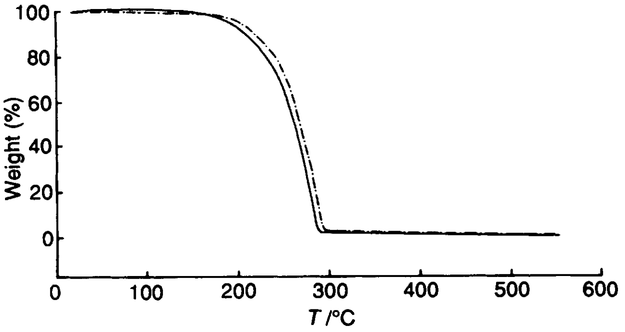

Fig. 2 Thermal gravimetric analysis plots for compound **1** (——) and its related hydrate (· — ·)

Finally, the DSC curve of compound **3** shows a melting point at 59 °C (−9.39 mcal mg^{-1}) and an irreversible decomposition at 270 °C. However, the hydrated starting compound exhibits rather different behaviour, having an endotherm at 114.37 °C (−6.31 mcal mg^{-1}), a melting point at 190.08 °C (−4.75 mcal mg^{-1}), and a further isotherm at 262.37 °C (−6.06 mcal mg^{-1}). The TGA shows a sublimation-onset temperature of 100 °C with completion by ≈312 °C. Over 97% of the material is vaporized leaving *ca.* 2% residue. In contrast, the TGA of the hydrate shows a higher onset temperature of 220 °C, with completion at approximately the same point as that of **3**, *i.e.* 318 °C.

As the precise nature of the compounds **1**–**3** could not be completely elucidated by spectroscopic methods, single-crystal X-ray structural studies were undertaken unambiguously to identify their structural compositions and to determine whether all the potential O-donor sites are bound to the metal centres.

X-Ray Determinations.—[{Eu(tmhd)$_3$}$_2$L^1] **1**. The crystal structure of complex **1** is shown in Fig. 3(*a*), with the methyl groups of the *tert*-butyls removed for clarity. Important bond distances and angles are listed in Table 3. The molecular structure consists of two Eu(tmhd)$_3$ moieties linked by a triglyme involving a unique bonding orientation. There is a 50:50 disorder in the orientation of the tmhd ligands around one of the europium atoms [Eu(2)] [see Experimental sections for details, and also Fig. 3(*b*)]. If one considers one of the pair of orientations of the tmhd ligands on Eu(2) the complex has an approximate, non-crystallographic, C_2 symmetry about an axis passing through the central ethylene bridge of the triglyme ligand [C(37) and C(38)].

Both metal centres are eight-co-ordinate, with the overall co-ordination polyhedron being distorted square antiprismatic (see Fig. 4), *cf.* [Eu(tmhd)$_3$(py)$_2$].[24] This co-ordination number is common for lanthanide alkoxides and β-diketones, *e.g.* [Y$_3$(OCH$_2$CH$_2$OMe)$_5$(acac)$_4$],[25] [Ln$_2$(tmhd)$_6$],[26] (Ln = La, Eu or Tb), [Eu(tmhd)$_3$(H$_2$O)][26] and [Y$_2$(O$_2$CMe)$_2$(acac)$_4$(H$_2$O)$_2$].[27] One of the most interesting features of complex **1** is the observation that the triglyme ligand acts as both a chelate and as a bridging ligand *via* the central ethylene bridge [C(37) and C(38)]. To the best of our knowledge this co-ordination mode of a glyme ligand is quite unique; such ligands are normally found either chelating or acting as terminally bound. This dinuclear structure does however permit the utilization of all four potential binding sites of the glyme ligand (*cf.* complex **3** below).

The Eu–O bond lengths [2.557(9)–2.653(9) Å] of the glyme ligand binding to the metal centre are an interesting example of the subtle steric factors involved in this unusual structural motif. The Eu(1)–O(34) bond length of 2.557(9) is *ca.* 0.1 Å shorter than that of Eu(1)–O(36) 2.653(9) Å, and this is most likely due to the fact that O(34) (carrying the pendant methyl group) can swing in and bind tightly to the metal centre. In striking contrast, O(36) must bend back on itself to create the chelate,

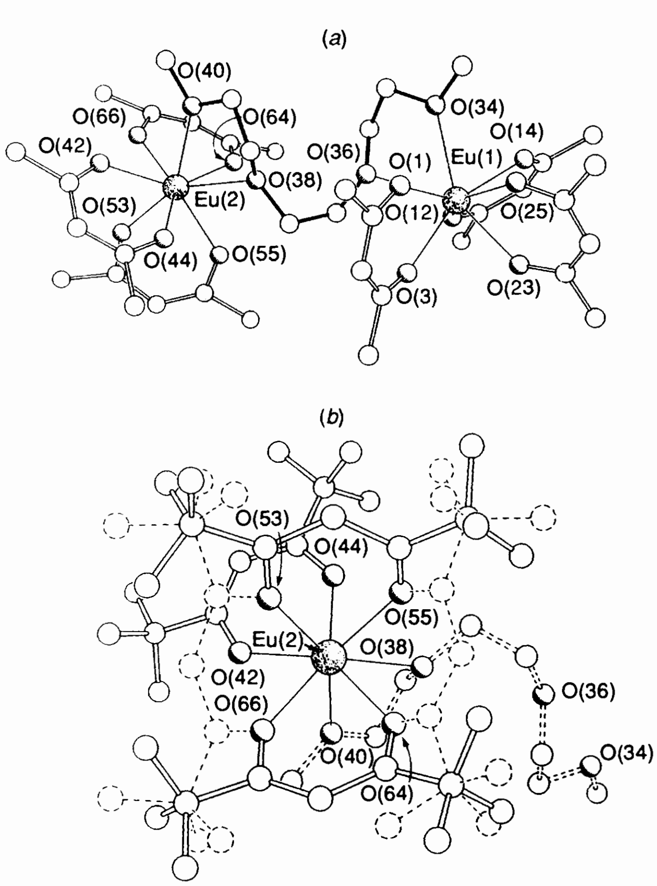

Fig. 3 (*a*) Molecular structure of $[\{Eu(tmhd)_3\}_2L^1]$ **1** showing the atom numbering scheme; Bu^t and hydrogen atoms have been omitted for clarity. (*b*) Part of the molecular structure of **1** illustrating the disorder in the co-ordination of the tmhd ligands about Eu(2). One orientation is illustrated with open bonds, while the other is indicated with dashed bonds and atoms

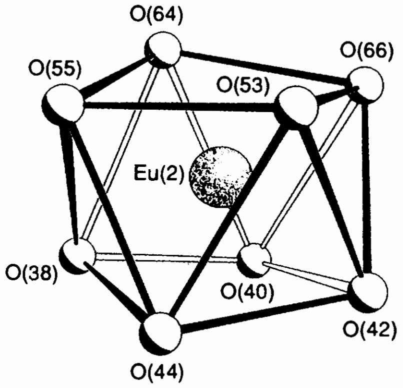

Fig. 4 Co-ordination polyhedron of $[\{Eu(tmhd)_3\}_2L^1]$ **1** showing the Eu(2) environment

with a fairly acute angle in the O(34)–Eu–O(36) plane of 61.6(3)°. Similar bonding is also observed at the other end of the glyme to Eu(2), with Eu(2)–O(38) and Eu(2)–O(40) 2.636(9) and 2.577(10) Å respectively, and O(38)–Eu(2)–O(40) 59.9(3)°.

There is retention of essentially *gauche* geometry about the C–C bonds within the glyme ligand, though there are notable departures from conventional *anti* geometries about some of the C–O linkages. This mode of binding of the glyme may also be contrasted with the use of functionalized alcohols (*e.g.* methoxyethanol) with yttrium which has yielded the crown-like decameric complex $[Y_{10}(OCH_2CH_2OMe)_{30}]$,[28] and the presence of Hacac produces $[Y_3(OCH_2CH_2OMe)_5(acac)_4]$.[25]

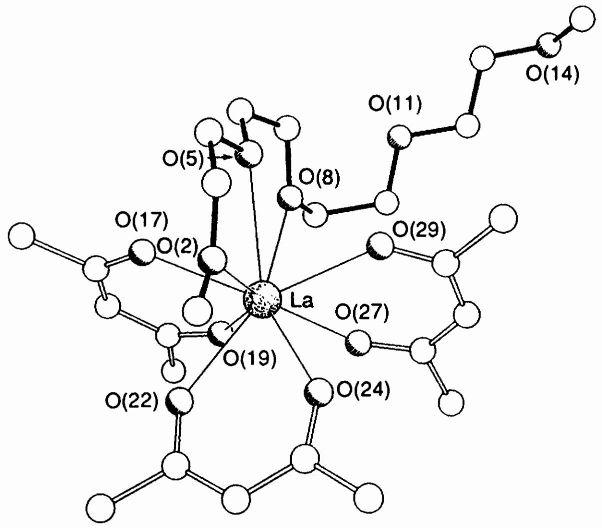

Fig. 5 Molecular structure of $[La(tmhd)_3L^2]$ **3** showing the atom numbering scheme; Bu^t and hydrogen atoms have been omitted for clarity

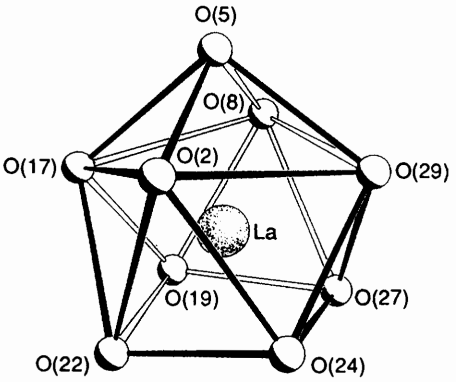

Fig. 6 Co-ordination polyhedron of $[La(tmhd)_3L^2]$ **3**

The Eu–O (of tmhd) bond lengths [2.256(9)–2.383(9) Å] are, as expected, much shorter than the Eu–O (of glyme) distances, given that the β-diketonates are observed here to be in a classical, nearly symmetrical mode. The Eu–O (of tmhd) bond lengths in **1** may also be compared with those in the complex $[Eu(tmhd)_3(py)_2]$[24] and also $[Eu(tmhd)_3(dmf)_2]$[29] (dmf = dimethylformamide) where average Eu–O (of tmhd) bond distances of 2.35 and 2.36 Å were observed.

$[\{Tb(tmhd)_3\}_2L^1]$ **2**. This compound is isostructural with complex **1** (see Experimental section).

$[La(tmhd)_3L^2]$ **3**. The structure of complex **3** is shown in Fig. 5. In contrast with **1**, this complex is monomeric, the stoichiometry being in clear agreement with the spectroscopic data. The lanthanum atom binds to all three bidentate tmhd ligands and to only three of the five possible oxygen atoms of the tetraglyme ligand. Thus the lanthanum atom clearly prefers to adopt a nine- rather than a possible eleven-co-ordination. The square-antiprismatic geometry of **1** is retained with the ninth co-ordinating oxygen atom [O(5)] capping one of the square faces (Fig. 6).

In this complex the co-ordinated portion of the tetraglyme chain has one short La–O bond, 2.706(7) Å [O(2)], and two long La–O bonds, 2.781(6) [O(5)] and 2.751(7) Å [O(8)]. The most noticeable and clearly unusual feature of complex **3** is the presence of the unco-ordinated portion of the tetraglyme chain C(9)–C(15) which, with the exception of the terminal methoxy bond, is approximately planar. This component of the ligand chain is rotated through *ca.* 70° about O(8)–C(9) relative to C(7)–O(8). The geometry of the co-ordinated portion of the glyme [O(2)–O(8)] retains the normal *gauche* and *anti* sequence about the C–C and C–O bonds.

A study of a space-filling model of complex **3** indicates that the co-ordination of an additional glyme oxygen centre is not favourable due to the presence of three tightly held tmhd ligands and with three of the five available glyme oxygen atoms saturating the lanthanum metal centre. However, it has recently been shown that when only two tmhd ligands are co-ordinated to a barium centre, *e.g.* [Ba(tmhd)$_2$L^2], all five oxygen atoms of the tetraglyme can be co-ordinated to the metal centre.[12] It is surprising in the light of the bridging arrangement observed for complex **1** that a similar utilization of the unco-ordinated oxygen centres [O(11) and O(14)] to form a dinuclear structure is not observed for **3**. A study of the packing of the monomers in the structure does not reveal any significant intermolecular/interchain interactions.

In this molecule the La–O bond distances fall into two distinctly different groups; those to the β-diketonate ligands, which lie in the range 2.403(6) [O(27)] to 2.495(6) Å [O(17)], and those for the tetraglyme, which are between 2.706(7) [O(2)] and 2.781(6) Å [O(5)]. These values are approximately 0.2 Å less than those observed for the recently characterized barium complexes, *e.g.* [Ba(tmhd)$_2$L^1] and [Ba(tmhd)$_2$L^2]. If compared with complex **1**, the bond lengths of **3** can be seen to be approximately 0.1 Å longer than the respective Eu–O (of glyme) or Eu–O (of tmhd) ligand bond lengths found in **1**. These differences are almost certainly in part due to the significantly different ionic radii of the metal centres involved [*i.e.* Ba^{2+} (1.37) > La^{3+} (1.06) > Eu^{3+} (0.85 Å)]. However, one must not ignore the effects of the steric bulk of the ligands involved.

Conclusion

The synthetic route described herein has been shown for the three complexes studied to be an efficient route to preparing water-free lanthanide β-diketonate complexes, from their corresponding hydrated materials. It is relatively simple, and involves the reaction of the glyme ligand (in near-stoichiometric amounts) in hexane with [Ln(tmhd)$_3$(H$_2$O)]. Our spectroscopic studies suggest that the glyme ligands act as a partitioning agent, removing the co-ordinated water *via* a chelate effect. The products obtained with either triglyme or tetraglyme have been shown to be air- and moisture-stable with excellent solubility in a wide range of organic solvents.

The DSC spectra for the complexes reveal a considerably reduced melting point. The TGA data show good thermal stability, which is nearly identical to that recorded for the hydrated complexes. Current precursors still suffer from poor long-term thermal stability in bubblers and we plan to study these phenomena by the use of modified TGA experiments, including the use of ramping experiments and holding the materials at a temperature halfway into the sublimation cycles for extended periods of time, also increasing the effective heating time, by changing the heating rate from 5 to 1 °C min^{-1}. The thermal behaviour and any residues can then be more properly assessed. Other future studies will include quantitative mass-transport studies and vapour-pressure measurements will be explored as part of our ongoing program into molecular precursors for metal oxide ceramics.

This strategy is potentially very powerful and may be used to stabilize a wide range of Ln–O complexes currently obtainable commercially as hydrated salts [*e.g.* LnX$_3$·H$_2$O, where X = halide, carboxylate, salicylate, nitrate, *etc.*]. Careful design of such precursors should yield great benefit to the metal–oxygen-based chemistry of these metals.

Acknowledgements

We thank the SERC for a studentship (D. J. O.) and for the X-ray diffractometers, the CASE sponsor Inorgtech (Dr. Tim Leedham) and for the Simultaneous Thermal Analysis equipment, and the Royal Society (for an inert-atmosphere glove-box).

References

1 R. C. Mehrotra, A. Singh and U. M. Tripathi, *Chem. Rev.*, 1991, **91**, 1287.
2 See: P. P. Edwards, M. R. Harrison and R. Jones, *Chem. Br.*, 1987, **23**, 962; M. O'Keefe and S. Hansen, *J. Am. Chem. Soc.*, 1988, **110**, 1506.
3 R. J. Cava, B. Ballog, J. J. Krajewski, L. W. Rupp, L. F. Schneemeyer, T. Siegrist, R. B. Van Dover, P. Marsh, P. K. Gallagher, S. H. Glarum, J. M. Marshall, R. C. Farrow, J. V. Waszczak, R. Hall and P. Trevor, *Nature (London)*, 1988, **336**, 211.
4 J. G. Bednorz and K. A. Müller, *Z. Phys. B, Condensed Matter*, 1986, **64**, 189.
5 H. Müller-Buschbaum, *Angew. Chem.*, 1989, **28**, 1472.
6 See, for example, J. R. McColl and F. C. Palilla, *ACS Symp. Ser.*, 1981, 177; G. Blasse, *Handbook on the Physics and Chemistry of Rare Earths*, eds. K. A. Gschneider and LeRoy Eyring, North Holland, Amsterdam, 1978, vol. 4, p. 237.
7 See, for example, J. Briggs, *Chem. Commun.*, 1970, 749.
8 D. C. Bradley, *Chem. Rev.*, 1989, **89**, 1317 and refs. therein.
9 See, for example, K. S. Mazdiyasni, C. T. Lynch and J. S. Smith, *Inorg. Chem.*, 1966, **3**, 342; K. S. Mazdiyasni and B. J. Schapar, *J. Less-Common Met.*, 1973, **30**, 105; R. C. Mehrotra and E. P. Gauer, *Metal β-diketonates*, Academic Press, London, 1978.
10 G. Urbain, *Bull. Soc. Chim.*, 1896, **15**, 338, 347; *C.R. Hebd. Seances Acad. Sci.*, 1897, **124**, 618; G. Urbain and A. Debierne, *C.R. Hebd. Seances Acad. Sci.*, 1899, **129**, 302.
11 T. Moeller and E. Schleiter-Rust, *Gmelin Handbook of Inorganic Chemistry, Sc, Y, La–Lu Rare Earth Elements Part D3*, 8th edn., Springer, Berlin, 1981.
12 See, for example, S. R. Drake, S. A. S. Miller and D. J. Williams, *Inorg. Chem.*, 1993, in the press; S. R. Drake, M. B. Hursthouse, K. M. A. Malik and S. A. S. Miller, *J. Chem. Soc., Chem. Commun.*, 1993, 478.
13 K. J. Eisentraut and R. E. Sievers, *J. Am. Chem. Soc.*, 1965, **87**, 5254.
14 SHELXTL version 4.2, Siemens X-Ray Analytical Instruments, 1991.
15 S. R. Drake, M. B. Hursthouse, D. J. Otway and K. M. A. Malik, *Inorg. Chem.*, 1993, in the press.
16 S. R. Drake, M. B. Hursthouse, D. J. Otway and K. M. A. Malik, unpublished work.
17 J.-H. So and P. Bodjouk, *Inorg. Chem.*, 1990, **29**, 1592.
18 H. Y. Lee, F. F. Cleveland, J. S. Ziomek and F. Jorke, *Appl. Spectrosc.*, 1972, **26**, 251.
19 See, for example, R. E. Sievers, *Nuclear Magnetic Shift Reagents*, Academic Press, New York, 1973.
20 T. H. Risby, P. C. Jurs, F. W. Lampe and A. L. Yergey, *Anal. Chem.*, 1974, **46**, 161; J. D. McDonald and J. L. Margrave, *J. Less-Common Met.*, 1968, **14**, 236.
21 J. Selbin, N. Ahmad and N. Bhacca, *Inorg. Chem.*, 1971, **10**, 1383.
22 M. S. Ansari and N. Ahmad, *J. Inorg. Nucl. Chem.*, 1975, **37**, 2099.
23 E. C. Ashby, P. Claudy, J. Bousquet and J. Etienne, *J. Chem. Educ.*, 1975, **52**, 618.
24 R. E. Cramer and K. Seff, *J. Chem. Soc., Chem. Commun.*, 1972, 400; *Acta Crystallogr., Sect. B*, 1972, **28**, 3281.
25 O. Poncelet, L. G. Hubert-Pfalzgraf and J.-C. Daran, *Inorg. Chem.*, 1990, **29**, 2885.
26 C. S. Erasmus and J. C. A. Boeyens, *Acta Crystallogr., Sect. B*, 1970, **26**, 1843.
27 O. Poncelet and K. G. Hubert-Pfalzgraf, *Polyhedron*, 1990, **9**, 1305.
28 O. Poncelet, L. G. Hubert-Pfalzgraf, J.-C. Daran and R. Astier, *J. Chem. Soc., Chem. Commun.*, 1989, 1846.
29 J. A. Cunningham and R. E. Sievers, *Inorg. Chem.*, 1980, **19**, 595.

Received 19*th February* 1993; *Paper* 3/01019H